

FEDSM-ICNMM2010-' 00* -

ELECTROSTATIC AND CAPILLARY EFFECTS ON THE DETACHMENT OF PARTICLES WITH SURFACE DEFORMATION IN TURBULENT FLOWS

Xinyu Zhang

Department of Mechanical and Aeronautical
Engineering
Clarkson University, Potsdam, NY 13699-5725
The United States
zhangxi@clarkson.edu

Goodarz Ahmadi

Department of Mechanical and Aeronautical
Engineering
Clarkson University, Potsdam, NY 13699-5725
The United States
ahmadi@clarkson.edu

ABSTRACT

Rolling detachment of micro particles in turbulent flows under the presence of electrostatic and capillary forces was studied. The maximum adhesion resistance model and the effective thermodynamic work of adhesion including the effects of electrostatic and capillary forces were used in the analysis. The JKR and DMT models for elastic interface deformations and the Maugis-Pollock model for the plastic deformation were extended to include the effect of electrostatic and capillary forces. The turbulence burst model was used to evaluate the airflow velocity near the substrate. The critical shear velocities for removal of particles of different sizes were evaluated and the results were compared with those without electrostatic and capillary forces. The relative critical shear velocities as well as the material dependence were also studied. The effect of the direction of the combined Coulomb force was also included. The predictions of the electric detachment fields for particles were compared with the available experimental data and good agreement was observed.

Keywords: Particle Adhesion; Particle Removal; Electrostatic Force; Capillary Force; Surface Tension; Resuspension; Elastic Deformation; Plastic Deformation.

INTRODUCTION

Micro-particle adhesion and removal have broad applications in semiconductor, pharmaceutical and xerographic industries. However, despite many prior studies [1-5], the electrostatic and capillary effects on particle adhesion and removal are not yet fully understood.

The electrostatic forces strongly affect the detachment of the charged particles in an electric field. Hays [6, 7] studied

the detachment of charged toner particles in an electric field. Mizes [8] reported the relative contributions of nonelectrostatic and electrostatic forces to the net particle adhesion force. Soltani and Ahmadi [9] performed a detailed study on rough particle detachment with electrostatic forces in turbulent flows. Their predictions agreed well with the experimental results obtained by Hays [6, 7] and Mizes [8].

The capillary force significantly affects the detachment of the particles in humid air. Zimon [10] and Taheri and Bragg [11] experimentally studied particle resuspension in dry and humid air conditions. Taheri and Bragg [11] conducted their experiments under the condition of normal room temperature and humidity, their results agree well with the simulation result obtained by Soltani and Ahmadi [12] for moist particle resuspension. Ibrahim et al. [13, 14] measured particle resuspension in both dry and humid air conditions. Ahmadi et al. [15] studied particle adhesion and detachment in turbulent flows including the effect of capillary forces. Zhang and Ahmadi [16] analyzed particle detachment with capillary force using a maximum adhesion resistance moment model. They developed an effective thermodynamic work of adhesion theory to include capillary force for particle adhesion and detachment in turbulent flows. More recently, Zhang and Ahmadi [17] studied particle detachment using an extended effective thermodynamic work of adhesion theory to include both capillary and electrostatic force for particles with an average Boltzmann charge distribution in turbulent flows.

In this study, the rolling detachment of spherical particles with saturation charge distribution in the presence of capillary and electrostatic forces was studied. An extended effective thermodynamic work of adhesion model proposed by Zhang and Ahmadi [17] was used to account for the effects of

capillary and electrostatic forces for hydrophilic materials. The maximum adhesion resistance moments were evaluated using the JKR and the DMT models for elastic surface deformation, and the Maugis-Pollock model for plastic surface deformation. The near-wall velocity field was evaluated by the turbulence burst/inrush model. The rolling detachment of spherical particles was investigated and the critical shear velocities for detaching particles of various sizes were evaluated. The material dependence and the effect of the direction of the combined Coulomb force were also studied. The results show that the capillary and electrostatic forces play major roles in the particle adhesion and detachment.

NOMENCLATURE

A	Hamaker constant
a	contact radius, m
a_e	effective contact radius, m
C_c	Cunningham factor
d	particle diameter, m
d_c	particle diameter in cgs units, cm
E	electric field strength in mks units, V/m
E_i	Young modulus of material i, N/m^2
e	electronic unit charge in mks units, C.
e_c	electronic unit charge in cgs units, stC.
F_c	capillary force, N
F_e	electrostatic force, N
F_{po}	pull-off force, N
F_t	drag force, N
H	hardness of material, Pa
Kn	Knudsen number
M_{Max}	maximum adhesion resistance moment due to the applied normal load, N·m
M_t	hydrodynamic moment, N·m
M_{Max}^{DMT}	maximum resistance moment evaluated by DMT model, N·m
M_{Max}^{JKR}	maximum resistance moment evaluated by JKR model, N·m
M_{Max}^{MP}	maximum resistance moment evaluated by Maugis-Pollock model, N·m
n	number of units of charge
$(P \cdot a)_{Max}$	maximum adhesion resistance moment, N·m
q	charges
u_c^*	minimum shear velocity needed for detaching a particle from the substrate, m/s
u^*	shear velocity, m/s

W_A	thermodynamic work of adhesion, J/m^2
W_A^c	effective thermodynamic work of adhesion, J/m^2
W_A^{eJKR}	effective thermodynamic work of adhesion for JKR model, J/m^2
W_A^{eDMT}	effective thermodynamic work of adhesion for DMT model, J/m^2
W_A^{eMP}	effective thermodynamic work of adhesion for Maugis-Pollock model, J/m^2

Greek letters

α	half particle-liquid contact angle, rad
α_o	overlap between the particle and surface, m
ϵ	dielectric constant of the particle, dimensionless.
ϵ_0	permittivity, F/m
θ	wetting angle, rad
λ	mean free path of air, m
ν_i	Poisson's ratio of material i
ρ	density of air, kg/m^3
ρ_p	density of particle and substrate material, kg/m^3
σ	surface tension of water, N/m

ADHESION MODELS

The adhesion models used in this study are similar to that used in Zhang and Ahmadi [16], the detailed information can be found in Zhang and Ahmadi [16].

CAPILLARY FORCE, ELECTROSTATIC FORCE AND EFFECTIVE THERMODYNAMIC WORK OF ADHESION

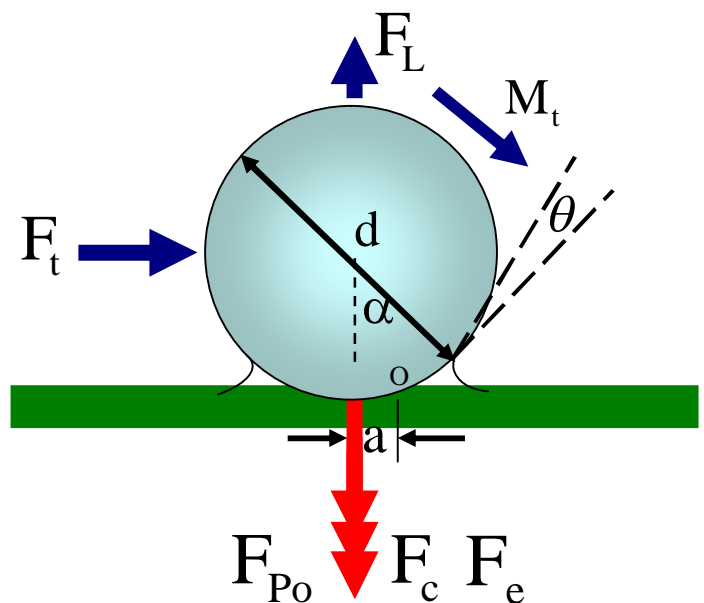


Figure 1. Geometric features of a spherical particle attached to a flat surface with capillary effect.

Capillary Force

As shown in Figure 1, for a particle and a flat surface made out of hydrophilic materials in humid air, the capillary force can be determined by the surface tension of water σ ($=0.0735$ N/m, at room temperature), the particle diameter d , the wetting angle θ and the angle α as:

$$F_c = 2\pi\sigma d[\sin\alpha \sin(\theta + \alpha) + \cos\theta]. \quad (1)$$

The angle α is in general very small, thus for small values of wetting angle θ , the final expression for the capillary force becomes:

$$F_c = 2\pi\sigma d. \quad (2)$$

Charge Distribution

Particles can be charged through three mechanisms: Boltzmann charging, diffusion charging and field charging. Boltzmann charging occurs for small particles in a bipolar ionic atmosphere. Diffusion charging occurs when uncharged particles obtain charges by diffusion of charged unipolar gaseous ions to their surfaces through random collisions between ions and particles. Field charging occurs when particles in an electric field acquire charges due to collisions with ions which are moving along the lines of force that intersect the particle surfaces. For a given charging condition after a sufficient time, the saturation number of charges n acquired by the particle of diameter d is given as [18]:

$$n = \left[\frac{3\varepsilon}{\varepsilon + 2} \right] \left[\frac{E_c d_c^2}{4e_c} \right], \quad (3)$$

where ε is the dielectric constant of the particle, d_c is particle diameter in cm, $e_c = 4.8 \times 10^{-10}$ stC (electrostatic units) is the electronic unit charge in cgs units, and E_c is the electric field strength in cgs units. Equations (3) is expressed in cgs units.

Electrostatic Force

For a charged particle sitting on a conducting substrate in an applied electric field, the electrostatic force acting on the particle is given by [9]

$$F_e = qE + \frac{q^2}{4\pi\varepsilon_0 d^2} + \frac{qE}{2} + \frac{3\pi\varepsilon_0 d^2 E^2}{8}. \quad (4)$$

Where $\varepsilon_0 = 8.859 \times 10^{-12}$ F/m is the permittivity. d is the particle diameter, E is the electric field strength, and q is the total electrical charges on the particle, which is given by [9]:

$$q = ne, \quad (5)$$

where $e = 1.6 \times 10^{-19}$ C is the electronic unit charge in mks units. n is the number of units of charges. The first term on the

right-hand side of equation (4) is Coulomb force. The second, third and fourth term is image force, dielectrophoretic force and polarization force, respectively.

In order to include the effects of capillary and electrostatic forces in adhesion models, it is reasonable to account for the combined effect of van der Waals adhesion, capillary and electrostatic forces with an effective thermodynamic work of adhesion W_A^e , which is variable with different adhesion models.

Effective Thermodynamic Work of Adhesion

To evaluate the effective thermodynamic work of adhesion for the JKR model, the effective pull-off force must be balanced with the combined effect of van der Waals pull-off force, the capillary and electrostatic forces. i.e.:

$$\frac{3}{4}\pi W_A^{eJKR} d = \frac{3}{4}\pi W_A d + F_c + F_e, \quad (6)$$

where W_A^{eJKR} is the effective work of adhesion for the JKR model. F_c and F_e are given by equations (2) and (4). Thus one has:

$$W_A^{eJKR} = W_A + \frac{8\sigma}{3} + \frac{2qE}{\pi d} + \frac{q^2}{3\pi^2\varepsilon_0 d^3} + \frac{\varepsilon_0 d E^2}{2}. \quad (7)$$

The corresponding approximate expression for the effective contact radius is then given with W_A being substituted by W_A^{eJKR} .

The effective thermodynamic work of adhesion for the DMT and the Maugis-Pollock models can be evaluated by a similar method. That is,

$$W_A^{eDMT} = W_A^{eMP} = W_A + 2\sigma + \frac{1.5qE}{\pi d} + \frac{q^2}{4\pi^2\varepsilon_0 d^3} + \frac{3\varepsilon_0 d E^2}{8} \quad (8)$$

ROLLING DETACHMENT MODEL

Ziskind et al. [19] reported a model for rolling detachment of a sphere from a surface, where the detachment starts when the hydrodynamic moment exceeds the maximum adhesion resistance moment evaluated for the JKR and DMT models for elastic surface deformations. Here the approach is extended to consider the effect of capillary and electrostatic forces as well as the effect of plastic surface deformation.

Figure 1 shows a spherical particle attached to a planar substrate in a fluid flow. The lift and gravity forces are very small, thus are neglected in this study. In humid air, a meniscus is formed at the particle-substrate contact. The particle will be detached when the moment of the hydrodynamic force about the point "O" (which is located at the rear perimeter of the contact circle) exceeds the maximum adhesion resistance moment due to combined adhesion,

capillary and electrostatic forces. That is:

$$M_t + F_t \left(\frac{d}{2} - \alpha_o \right) \geq (P \cdot a)_{\text{Max}} \quad (9)$$

where F_t is the fluid drag force, α_o is the relative approach between the particle and surface, M_t is the hydrodynamic moment about the center of the particle, $(P \cdot a)_{\text{Max}}$ is the maximum adhesion resistance moment due to combined adhesion, capillary and electrostatic forces. In most practical cases, α_o is very small and can be neglected and Equation (9) becomes:

$$M_t + F_t \frac{d}{2} \geq (P \cdot a)_{\text{Max}} \quad (10)$$

MAXIMUM ADHESION RESISTANCE

The maximum adhesion resistance moment can be evaluated by a similar approach as developed by Zhang and Ahmadi [16]. In this study, the JKR and DMT adhesion models are used for elastic surface deformations, while the Maugis-Pollock adhesion model is used for plastic surface deformation.

For the JKR model with capillary and electrostatic forces

$$M_{\text{Max}}^{\text{JKR}} = 2.707 \frac{W_A^{\text{eJKR}} d^{4/3} d^{5/3}}{K^{1/3}} \quad (11)$$

For the DMT model with capillary and electrostatic forces

$$M_{\text{Max}}^{\text{DMT}} = 1.725 \frac{W_A^{\text{eDMT}} d^{4/3} d^{5/3}}{K^{1/3}} \quad (12)$$

For the Maugis-Pollock model with capillary and electrostatic forces

$$M_{\text{Max}}^{\text{MP}} = \frac{2\pi(W_A^{\text{eMP}} d)^{3/2}}{3\sqrt{3}H} \quad (13)$$

HYDRODYNAMIC FORCES AND TORQUES

Soltani and Ahmadi [12, 20] suggested that the particle detachment process is strongly affected by the near-wall burst and inrush processes. Based on the burst/inrush model, the drag force acting on the particle is given by:

$$F_t = \frac{4.38\pi\rho d^2 u^{*2}}{C_c} \quad (14)$$

where ρ is the density of the air and C_c is the Cunningham factor given by [21, 22]:

$$C_c = 1 + \text{Kn} [1.257 + 0.4\exp(-1.1/\text{Kn})] \quad (15)$$

Here the Kn is the Knudsen number given as:

$$\text{Kn} = \frac{2\lambda}{d} \quad (16)$$

where λ is the mean free path of air.

The corresponding moment of the hydrodynamic force

acting on the particle can be evaluated as:

$$M_t = \frac{1.62\pi\rho u^{*2} d^3}{C_c} \quad (17)$$

PARTICLE DETACHMENT

The critical shear velocity can be obtained by substituting the expression for the hydrodynamic drag and torque into Equation (10):

$$u_c^{*2} = \frac{M_{\text{Max}}}{3.81\pi\rho d^3/C_c} \quad (18)$$

where M_{Max} is the maximum adhesion resistance moment as shown in Equations (11), (12) and (13), respectively.

Comparison with Experimental Data

Figure 2 shows the comparison of the critical electric detachment fields by JKR model with the experimental data of Hays [6] for 13 μm toner (PSL) particles on a nickel carrier bead without flow and capillary effects. This figure is included in previous work [17]. It is listed here again for convenience. Here Coulomb force and dielectrophoretic force are directed away from the substrate. It shows that the critical electric detachment fields increases with the increase of the charges

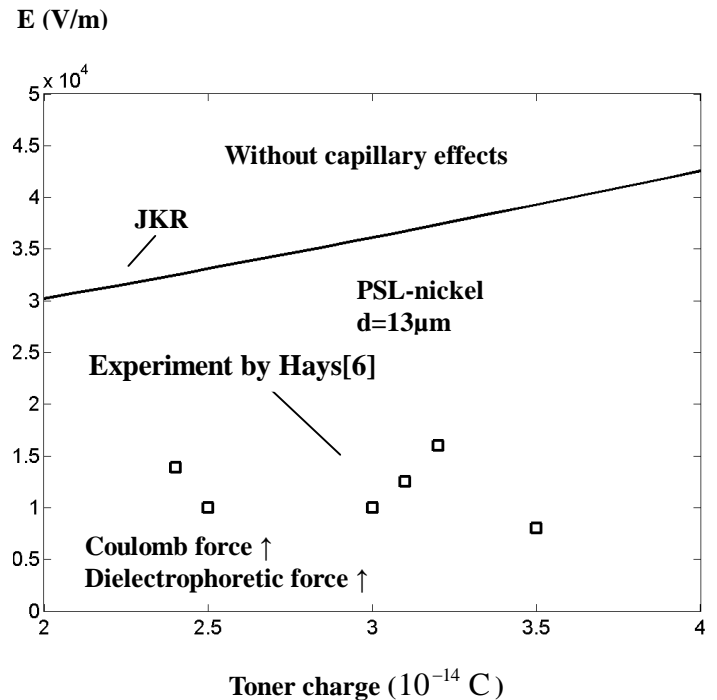


Figure 2. Comparison of the electric detachment fields for particles with the experimental data of Hays [6] for toner (PSL) particles on a nickel carrier bead without flow and capillary effects. Coulomb force and dielectrophoretic force are directed away from the substrate.

carried by the particles. It also shows that the predicted electric detachment fields from the JKR model are higher than the experimental data. This is because that the toner particles are not smooth particles; the coarse surface roughness of the toner particles will decrease the particle adhesion force and therefore decrease the electric detachment fields.

RESULTS

In this section the results are presented and discussed. The material properties are listed in Table 1. Two electric fields are used in the study, 5000 kV/m and 10000kV/m. The results are presented in term of critical shear velocity, u_c^* , which is the minimum shear velocity needed to remove a particle from the substrate.

Table 1. Material properties for different combinations

Material combination	E	A	W_A	ρ_p	ν_i	H
Polystyrene-polystyrene	0.28	6.4	10.56	1.05	0.33	6.6
Glass-glass	6.9	8.5	14.1	2.18	0.2	490-665.4
Polystyrene-nickel	–	–	23.65	–	–	–

E: Young's modulus of material, (10^{10} Pa)

A: Hamaker constant, (10^{-20} J)

W_A : thermodynamic work of adhesion, (10^{-3} J/m²)

ρ_p : density of material, (10^3 kg/m³)

ν_i : Poisson's ratio of material i

H: hardness of material, (10^7 Pa)

Figure 3 shows the variations of u_c^* with particle diameter predicted by different adhesion models in two electric fields for the rolling detachment of polystyrene particles with saturation charge distribution from a polystyrene substrate in dry conditions. Here Coulomb force and dielectrophoretic force are directed towards the substrate. It can be seen that the critical shear velocity decreases with the increase of the

particle diameter, which implies that compared to larger particles, small particles are more difficult to remove. It also can be seen that the critical shear velocity predicted by the JKR adhesion model is the largest. The predicted value by the Maugis-Pollock model, which accounts for plastic deformation, is the lowest. The differences are small for smaller particles, but become relatively large for larger particles. As suggested by Zhang and Ahmadi [16], these differences are due to the variations of the maximum adhesion resistance moments for the JKR, DMT and Maugis-Pollock models. Figure 3 also shows that the critical shear velocities in an electric field of 5000 kV/m are lower than those in 10000kV/m. The differences are small for smaller particles, but become large for larger particles. The reason is that the electrostatic forces increase with the increase of electric field intensity, and larger particles carry more charges, as seen from equation (3).

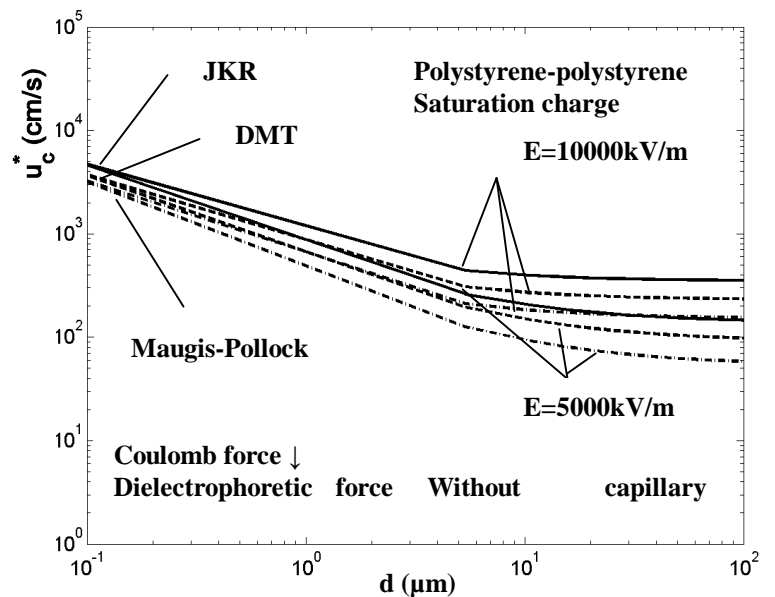


Figure 3. Variation of the critical shear velocities with the particle diameter for resuspension of polystyrene particles with saturation charge distribution from a polystyrene substrate without capillary effects.

Figure 4 shows the variations of u_c^* with particle diameter as predicted by different adhesion models in the presence of capillary effects and different electric fields for the rolling detachment of polystyrene particles with saturation charge distribution from a polystyrene substrate. Here Coulomb force and dielectrophoretic force are directed to the substrate. It can be seen that the critical shear velocity decreases with the increase of the particle size. The model predictions from the JKR model are slightly higher than those from the DMT model. The predictions from the Maugis-Pollock model for u_c^* are the lowest for large particles, but slightly higher than those

from the DMT model for small particles. Compared to the results presented in Figure 3, Figure 4 shows much higher critical shear velocities. This implies that the capillary force significantly increases the critical shear velocity. Figure 4 also shows that the critical shear velocities in an electric field of 5000 kV/m are lower than those in 10000kV/m, but the differences are relatively smaller compared to the results presented in Figure 3. This proves that when Coulomb force and dielectrophoretic force are directed towards the substrate, the relative effects of the electrostatic forces decrease in the presence of capillary effects.

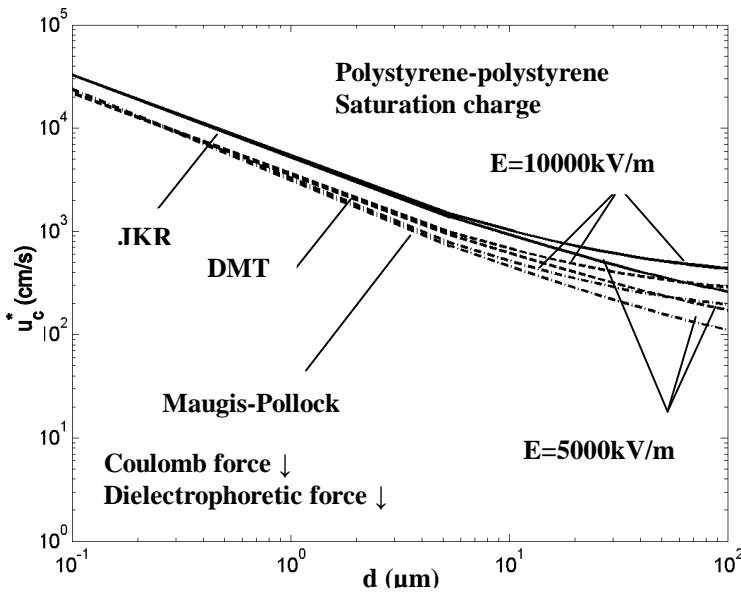


Figure 4. Variation of the critical shear velocities with the particle for resuspension of polystyrene particles with saturation charge distribution from a polystyrene substrate in the presence of capillary effects.

Figure 5 shows the comparison of u_c^* for the cases with or without capillary effects predicted by different adhesion models for the rolling detachment of polystyrene particles from a polystyrene substrate without electrostatic forces. It can be seen that the capillary effects significantly increase the critical shear velocity. Comparing Figure 5 with Figures 3 and 4, one can find that the electrostatic forces only have major effects on large particles. When Coulomb force and dielectrophoretic force are directed to the substrate, the electrostatic forces can significantly increase the critical shear velocity for large particle detachment.

Figure 6 shows the variations of u_c^* with particle diameter as predicted by different adhesion models in the presence of capillary effects and different electric fields for the rolling detachment of glass particles with saturation charge distribution from a glass substrate. Here the Coulomb and dielectrophoretic forces are directed towards the substrate. The trends are similar to those observed in Figure 4. Figure 6

shows that the critical shear velocity decreases with the increase of the particle diameter. The model predictions from the JKR model are higher than those from the DMT model. The predictions from the Maugis-Pollock model are the lowest. The critical shear velocities in an electric field of 5000 kV/m are lower than those in 10000kV/m. Compared to Figure 4, Figure 6 shows lower critical shear velocities. This implies that for particles with saturation charge distribution, detaching glass particles from a glass substrate is easier than detaching polystyrene particles from a polystyrene substrate.

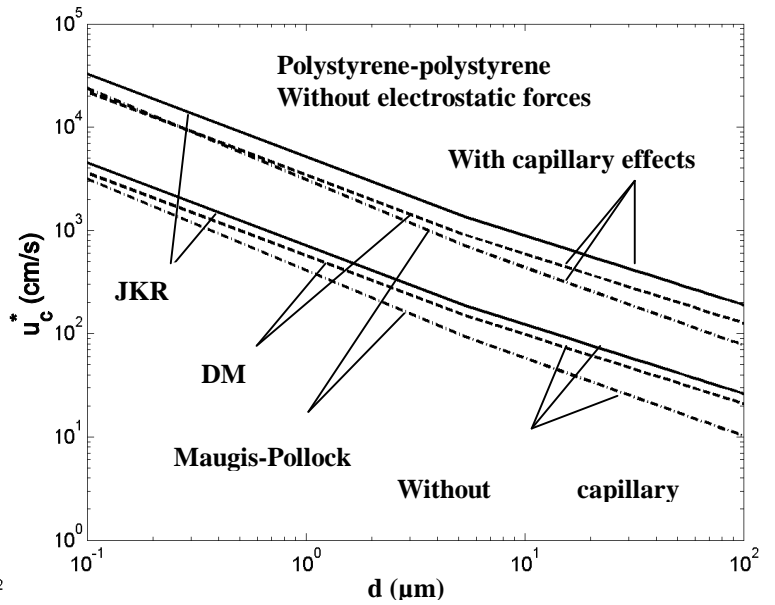


Figure 5. Variation of the critical shear velocities with the particle diameter for resuspension of polystyrene particles from a polystyrene substrate without electrostatic effects.

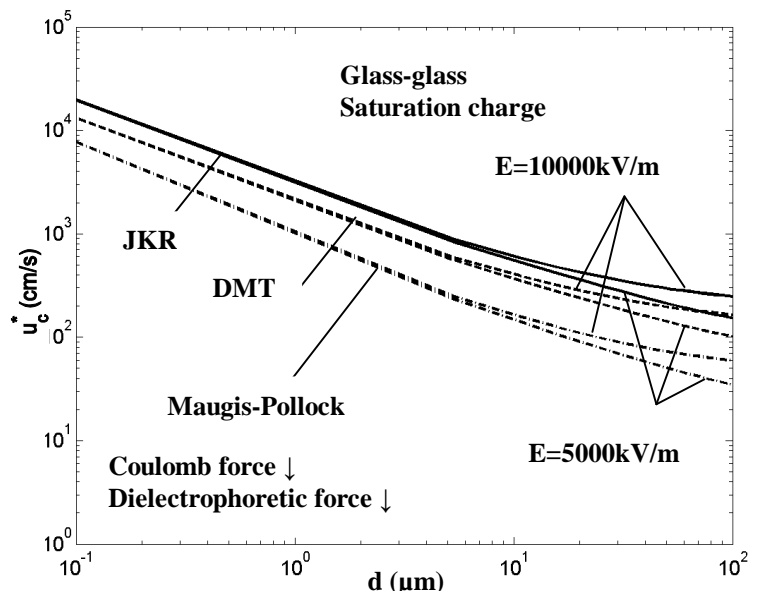


Figure 6. Variation of the critical shear velocities with the particle diameter for resuspension of glass particles with saturation charge distribution from a glass substrate in the presence of capillary effects.

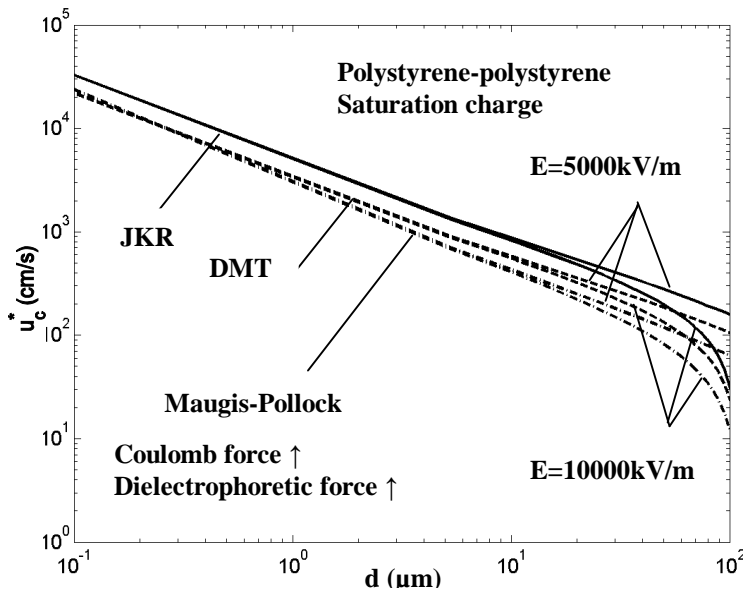


Figure 7. Variation of the critical shear velocities with the particle diameter for resuspension of polystyrene particles with saturation charge distribution from a polystyrene substrate in the presence of capillary effects. Coulomb force and dielectrophoretic force are directed away from the substrate.

Figure 7 shows the variations of u_c^* with particle diameter as predicted by the different adhesion models in the presence of capillary effects and different electric fields for the rolling detachment of polystyrene particles with saturation charge distribution from a polystyrene substrate. Here the Coulomb and dielectrophoretic forces are directed away from the substrate. Figure 7 shows that the critical shear velocity decreases with the increase of the particle diameter. The model predictions from the JKR model are slightly higher than those from the DMT model. The predictions from the Maugis-Pollock model for u_c^* are the lowest for large particles, but slightly higher than those from the DMT model for small particles. Compared to results presented in Figure 4, Figure 7 shows lower critical shear velocities for large particles, especially in an electric field of 10000 kV/m. This implies that in the presence of capillary force, when directed away from the substrate and under a strong electric field, Coulomb force and dielectrophoretic force significantly decrease the critical shear velocity for large particle rolling removal. Figure 7 also shows that the critical shear velocities in an electric field of 5000 kV/m are higher than those in 10000kV/m, and the differences are relatively larger compared to results presented in Figure 4, where Coulomb force and dielectrophoretic force are directed

towards the substrate. This means that the relative effects of the electrostatic forces increase when Coulomb force and dielectrophoretic force are directed away from the substrate.

CONCLUSIONS

Particle resuspension including the effects of capillary and electrostatic forces for hydrophilic materials was studied. The effective thermodynamic work of adhesion theory including the effects of electrostatic and capillary forces was used in the analysis. The JKR, DMT and Maugis-Pollock models were extended to include the effect of electrostatic and capillary forces. The critical shear velocities to detach particles of different sizes were evaluated. The material dependence and the effect of the direction of the combined Coulomb force were also analyzed. The predictions of the electric detachment fields for particles were compared with the experimental data. Based on the presented results the following conclusions are obtained:

- The capillary force significantly increases the critical shear velocity for particle detachment; while the electrostatic forces only have major effects for large particles.
- When Coulomb force and dielectrophoretic force are directed towards the substrate, the electrostatic forces can increase the large particle's critical shear velocity, but the relative effects of the electrostatic forces will decrease in the presence of capillary effects.
- In the presence of capillary force, when Coulomb force and dielectrophoretic force are directed away from the substrate under a strong electric field, Coulomb force and dielectrophoretic force can significantly decrease the critical shear velocity for large particle rolling detachment.
- For particles with saturation charge distribution, detaching glass particles from a glass substrate is easier than detaching polystyrene particles from a polystyrene substrate.

ACKNOWLEDGMENTS

The financial support of the Environmental Protection Agency (EPA) and the NYSTAR Center of Excellence at Syracuse University is gratefully acknowledged.

REFERENCES

1. H. Krupp, 1967, Particle adhesion: Theory and experiment, *Adv. Colloid Interface Sci.* **1**, 111-140.
2. J. Visser, 1972, On Hamaker constants: a comparison between Hamaker constants and Lifshitz-Van der Waals constant, *Adv. Colloid Interface Sci.* **3**, 331-363.
3. D. Tabor, 1977, Surface forces and surface interactions, *J. Colloid Interface Sci.* **58**, 2-13.

4. R. A. Bowling, 1985, An analysis of particle adhesion on semiconductor surfaces, *J. Electrochem. Soc. Solid State Science Technol.* **132**, 2208- 2219.
5. R. C. W. Berkeley, *Microbial Adhesion to Surfaces*, pp. 93-113, Ellis Horwood, New York (1980).
6. D. A. Hays, 1978, Electric field detachment of toner, *Photogr. Sci. Eng.* **22**. 232-235.
7. D. A. Hays and W. H. Wayman, 1983, Adhesion of charged particles, *Electrostatics Inst. Phys. Conf. Ser. No. 66*. p. 237-242. The Institute of Physics. London.
8. H. A. Mizes, 1994, Adhesion of small particles in electric field, *J. Adhesion Sci. Technol.* **8**. 937-953.
9. M. Soltani and G. Ahmadi, 1999, Detachment of rough particles with electrostatic attraction from surfaces in turbulent flows, *J. Adhesion Sci. Technol.* Vol. **13**, No. 3. pp325-355.
10. A.D. Zimon, 1982, *Adhesion of dust and powder*, Consultants Bureau, New York.
11. M. Taheri and G.M. Bragg, 1992, A study of particle resuspension in a turbulent flow using a preston tube, *Aerosol Sci. Technol.*, **15**, 15-20.
12. M. Soltani and G. Ahmadi, 1994, On particle adhesion and removal mechanisms in turbulent flows, *J. Adhesion Sci. Technol.*, **8**,763-785.
13. A.H. Ibrahim, P.F. Dunn, and R.M. Brach, 2003, Microparticle detachment from surfaces exposed to turbulent air flow: controlled experiments and modeling, *J. Aerosol Sci.***34**, 765-782.
14. A. H. Ibrahim , P. F. Dunn, and R. M. Brach, 2004, Microparticle detachment from surfaces exposed to turbulent air flow: Effects of flow and particle deposition characteristics *J. Aerosol Sci.*, **35**, 805-821.
15. G. Ahmadi, S. Guo and X. Zhang, 2007, Particle adhesion and detachment in turbulent flows including capillary forces, *Particulate Sci. Technol.* **25**: 1-18.
16. X. Zhang, G. Ahmadi, 2007, Rolling particle removal in turbulent flows-effects of capillary and deformation, *J. Adhesion Sci. Technol.* **21**, 1589-1611.
17. X. Zhang, G. Ahmadi, 2009, Micro Particles Detachment in Turbulent Flows with Electrostatic and Capillary Effects and Surface Deformation, *Proceedings Of FEDSM2009, 2009 ASME Fluids Engineering Summer Meeting, August 2-5, Vail Cascade Resort and Spa in Vail, Colorado.*
18. W. C. Hinds, 1982, *Aerosol Technology: Properties, Behavior, and Measurement of Airborne Particles*, John Wiley and Sons, New York.
19. G. Ziskind, M. Fichman and C. Gutfinger, 1997, Adhesion moment model for estimating particle detachment from a surface, *J. Aerosol Sci.* **28**, 623-634.
20. M. Soltani and G. Ahmadi, 1995, Particle detachment from rough surfaces in turbulent flows *J. Adhesion*, **51**, 105-123.
21. N. A. Fuchs, 1964, *The mechanics of aerosols*, MacMillan, New York.
22. S. K. Friedlander, 1977, *Smoke, dust and haze*, John Wiley, New York.